Lab on a Chip

Accepted Manuscript

This is an *Accepted Manuscript*, which has been through the RSC Publishing peer review process and has been accepted for publication.

Accepted Manuscripts are published online shortly after acceptance, which is prior to technical editing, formatting and proof reading. This free service from RSC Publishing allows authors to make their results available to the community, in citable form, before publication of the edited article. This *Accepted Manuscript* will be replaced by the edited and formatted *Advance Article* as soon as this is available.

To cite this manuscript please use its permanent Digital Object Identifier (DOI®), which is identical for all formats of publication.

More information about *Accepted Manuscripts* can be found in the **Information for Authors**.

Please note that technical editing may introduce minor changes to the text and/or graphics contained in the manuscript submitted by the author(s) which may alter content, and that the standard **Terms & Conditions** and the **ethical guidelines** that apply to the journal are still applicable. In no event shall the RSC be held responsible for any errors or omissions in these *Accepted Manuscript* manuscripts or any consequences arising from the use of any information contained in them.

RSC Publishing

www.rsc.org/loc
Registered Charity Number 207890

Microfluidic Micropipette Aspiration for Measuring the Deformability of Single Cells

Quan Guo, Sunyoung Park, and Hongshen Ma

Microfluidic device for measuring the deformability of single cells using threshold deformation pressure through micro-scale constrictions similar to micropipette aspiration

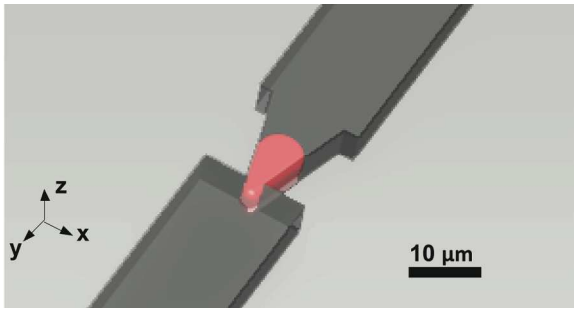

Microfluidic Micropipette Aspiration for Measuring the Deformability of Single Cells

Quan Guo[a], Sunyoung Park[a], and Hongshen Ma[a,b,c]

[a] *Department of Mechanical Engineering, University of British Columbia, 2054-6250 Applied Science Lane, Vancouver, BC, Canada V6T 1Z4*
[b] *Department of Urologic Science, University of British Columbia, Vancouver, BC, Canada*
[c] *Vancouver Prostate Centre, Vancouver General Hospital, Vancouver, BC, Canada*

Abstract

We present a microfluidic technique for measuring the deformability of single cells using the pressure required to deform such cells through micrometer-scale tapered constrictions. Our technique is equivalent to whole-cell micropipette aspiration, but involves considerably simpler operation, less specialized equipment, and less technical skill. Single cells are infused into a microfluidic channel, and then deformed through a series of funnel-shaped constrictions. The constriction openings are sized to create a temporary seal with each cell as it passes through the constriction, replicating the interaction with orifice of a micropipette. Precisely controlled deformation pressures are generated using an external source and then attenuated 100:1 using an on-chip microfluidic circuit. Our apparatus is capable of generating precisely controlled pressures as small as 0.3 Pa in a closed microchannel network, which is impervious to evaporative losses that normally limit the precision of such equipment. Intrinsic cell deformability, expressed as cortical tension, is determined from the threshold deformation pressure using the liquid-drop model. We measured the deformability of several types of nucleated cells and determined the optimal range of constriction openings. The cortical tension of passive human neutrophils was measured to be 37.0 ± 4.8 pN/µm, which is consistent with previous micropipette aspiration studies. The cortical tensions of human lymphocytes, RT4 human bladder cancer cells, and L1210 mouse lymphoma cells were measured to be 74.7 ± 9.8, 185.4 ± 25.3, and 235.4 ± 31.0 pN/µm respectively. The precision and usability of our technique demonstrates its potential of as a biomechanical assay for wide-spread use in biological and clinical laboratories.

Introduction and Background

The mechanical deformability of single cells can be used to evaluate the status of a wide range of diseases including cancer [1-3], malaria [3-5], and arthritis [6, 7]. Micropipette aspiration (MPA) is a highly effective technique for these studies and has been used to measure the deformability of erythrocytes [8, 9], leukocytes [10-14], chondrocytes [7], endothelial cells [15, 16], and epithelial cells

[11-14, 17]. The classical form of this technique involves the complete or partial suction of single cells into the orifice of a glass micropipette using a small negative pressure [10, 12, 18-22]. The intrinsic mechanical properties of aspirated cells can then be determined using various models based on the measured relationship between the suction pressure, the diameter of the pipette orifice, the diameter of the undeformed cell, and in the case of partial suction, the protrusion length of the cell in the pipette [10, 12, 18].

While conceptually straightforward, traditional MPA involves delicate procedures performed by highly skilled technicians using specialized equipment. As a result, MPA is largely used as a technique for fundamental biophysical studies, rather than as a biomechanical assay for wide-spread use in biological or clinical laboratories. The equipment for MPA experiments consists of a precision pressure generator, a 3-axis micro-manipulator, and a microscopy imaging system [18, 23, 24]. A typical measurement process involves initially installing a pipette and aligning the pipette tip with the focal plane of the microscopy system. Next, each target cell is located by microscopic inspection and aligned to the pipette tip. Finally, the target cell is aspirated into the pipette using a variable negative pressure while the resulting geometry of the cell is recorded and analyzed.

There are a number of technical challenges that make MPA experiments both challenging and time-consuming to perform. First, the aspiration of single cells requires extremely small and precise pressures, typically less than 100 Pa with an adjustment resolution of 0.1 Pa. At these pressures, conventional instruments can be compromised as a result of mechanical vibration, temperature and humidity fluctuations, as well as electronic noise and offsets [18]. Second, the alignment of the pipette tip with the focal plane of the imaging system, as well as the surface of the target cells is a manual process that requires considerable experimental skills and experience. Third, MPA experiments are performed in open-air conditions where the sample liquid is continuously lost due to evaporation. This slow volume change results in a drifting baseline of the aspiration pressure that must be corrected by periodic recalibration[18]. This procedure constrains the time available to aspirate each target cell, as well as the minimum sample volume. Finally, since the pipette is unchanged for the duration of each experiment, the test cells are deformed different amounts depending on their size. This constraint adds considerable experimental uncertainty to whole-cell aspiration studies where deformation pressures are typically highly sensitive to the degree of deformation.

Microfabrication and microfluidics technologies present new capabilities for creating structures at the length scale of individual cells and new methods for precisely controlling the flows of minute volumes of

liquid. Recently, a number of microfluidic techniques that leverage these capabilities have been developed for the study of cell biomechanics. Specifically, the deformability of single cells has been measured in these systems using transit time through constrictions [25-29], protrusion in constrictions [30-33], wedging in tapered constrictions [32, 33], elongation using fluid shear stress [34-36], and elongation using optical stress [1]. These approaches, however, have not been able to show a similar level of measurement precision as traditional MPA. Using the coefficient of variation (CV, ratio of standard deviation and mean) of the measured results as a metric for precision, MPA measurements of a single cell population typically report CVs from 0.1 to 0.25 [10, 24, 37], whereas results from existing microfluidic techniques show broad variation with CVs from 0.3 and 0.5 [1, 26-36].

In this paper, we present a microfluidic technique for measuring the deformability of single cells that is equivalent to whole-cell MPA with a similar level of precision, but offer dramatically simplified operation, improved ease-of-use, and improved robustness to errors. Key features of this device include the generation of precisely controlled pressures using fluidic circuitry, the ability to aspirate single cells using an enclosed device to eliminate evaporative losses, and the ability to perform experiments using multiple constrictions on the same cell.

Device Principles

Our technique measures cell deformability using the pressure required to deform individual cells through funnel-shaped constrictions as shown in Fig. 1. The funnel shape reduces the geometrical uncertainty associated with the fabrication of sharp corners and provides test cells with a smooth transition to deform through. Individual test cells, suspended in a fluid, are initially introduced into a microchannel and carried towards the constriction by the fluid as shown in Fig. 1B. During this period, the cell is hydrodynamically indistinguishable from the fluid, and the pressure difference applied across the channel (P_{ch}) is distributed across the entire microchannel. When the cell arrives at the constriction, it blocks the flow of the fluid, and dramatically increases the hydrodynamic resistance of the constriction (R_{funnel}) relative to that of the channel (R_{ch1} and R_{ch2}). As a result, the pressure difference applied across the channel is concentrated across the funnel constriction, such that $P_{ch} \simeq P_{funnel}$, as shown in Fig. 1C. Varying the pressure applied across the channel during this period enables different deformation pressures to be applied to a single cell. Previously, we used this mechanism to measure the directional asymmetry in the deformation of single cells across various funnel constrictions [38], and to study the stiffening of red blood cells parasitized by *P. falciparum* [39]. In this paper, we generalize this technique

for measuring the deformability of nucleated cells and present its potential to replace micropipette aspiration in these studies.

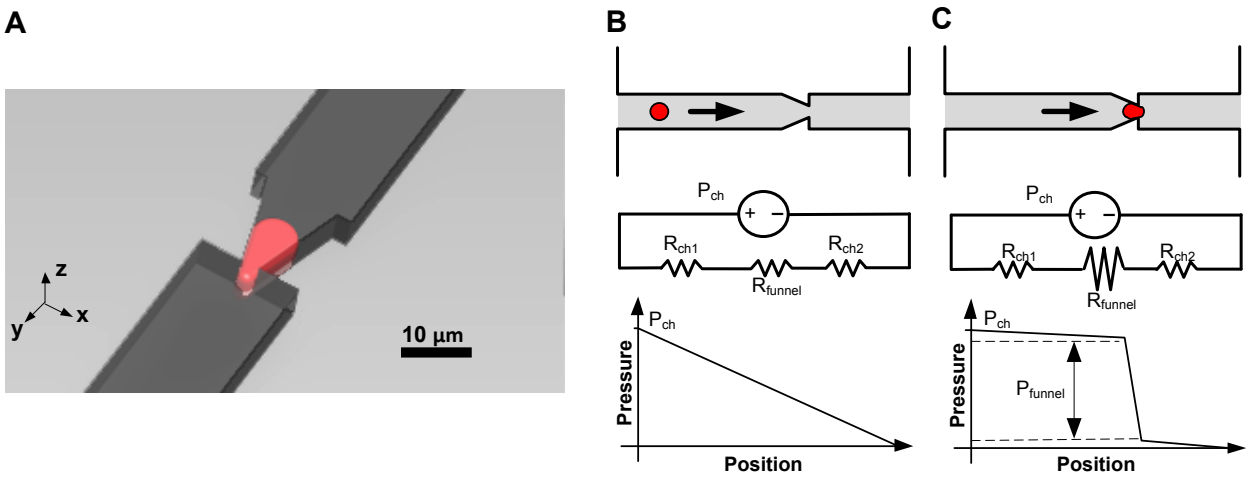

Fig. 1 *(A) A single cell being deformed through a funnel constriction. Pressure profiles of a microchannel containing (B) a free-flowing cell and (C) a cell constrained in a funnel constriction.*

The microfluidic device designed to deform single cells using precisely controlled pressure is a two-layer silicone microstructure fabricated using multi-layer soft lithography (Fig. 2) [40]. Test cells are introduced into an upper flow layer, where fluid flow is controlled by applying pressures to a lower control layer to actuate membrane microvalves formed at the intersection of flow and control layers. The flow layer consists of three microchannel networks including (i) funnel constrictions, (ii) pressure attenuator, and (iii) cell inlet. These three microchannel networks are isolated from each other using membrane microvalves, S1 through S4.

The funnel constrictions in which single cells are deformed through contain sidewalls angled at ±15°. The size of these funnel constrictions are defined by the minimum width or pore size (W_0) and the thickness of the microchannel (h_0). In the microfluidic device, the funnel constrictions are arranged in series with decreasing W_0 values ranging from 10 down to 1.2 µm. This arrangement allows each cell to be tested using several constrictions to select a range that achieves optimal cell compression. This arrangement further enables bracketing of the photolithographic fabrication process where over- or under-exposure can alter the final funnel geometry.

The pressure attenuator reduces an external pressure (P_{ab}) and applies it across the chain of funnel constrictions (P_{ch}). This capability is achieved using the hydrodynamic equivalent of a resistive divider electronic circuit. As shown in Fig. 2 (B), an external pressure is applied across a long channel between

points (a) and (b). A segment of this microchannel between the points (c) and (d), is spaced at 1/100 of its total length between (a) and (b). The chain of funnel constrictions is attached as an alternate branch to points (c) and (d). As long as the hydrodynamic resistance of this branch microchannel network is significantly greater than the hydrodynamic resistance between (c) and (d), the pressure difference between (c) and (d) is defined by its length ratio with (a) and (b). Specifically, the pressure between (c) and (d), P_{cd}, is 1/100 of the applied pressure between (a) and (b), P_{ab}.

The sensitivity of the deformation pressure measurement is therefore a function of the attenuation provided by the pressure divider and the precision of the external pressure source. We used a pressure controller (Fluigent, Paris, France) with a resolution of 30 Pa, which enables the microfluidic device to measure deformation pressures with a resolution of 0.3 Pa. Smaller pressures can be easily achieved using a pressure divider with greater attenuation ratio or using a more precise pressure controller. Since the attenuated pressure dramatically reduces the flow rate of fluid through the funnel chain, a separate cell inlet is necessary to first introduce single cells into the funnel chain region before the pressure measurement could take place.

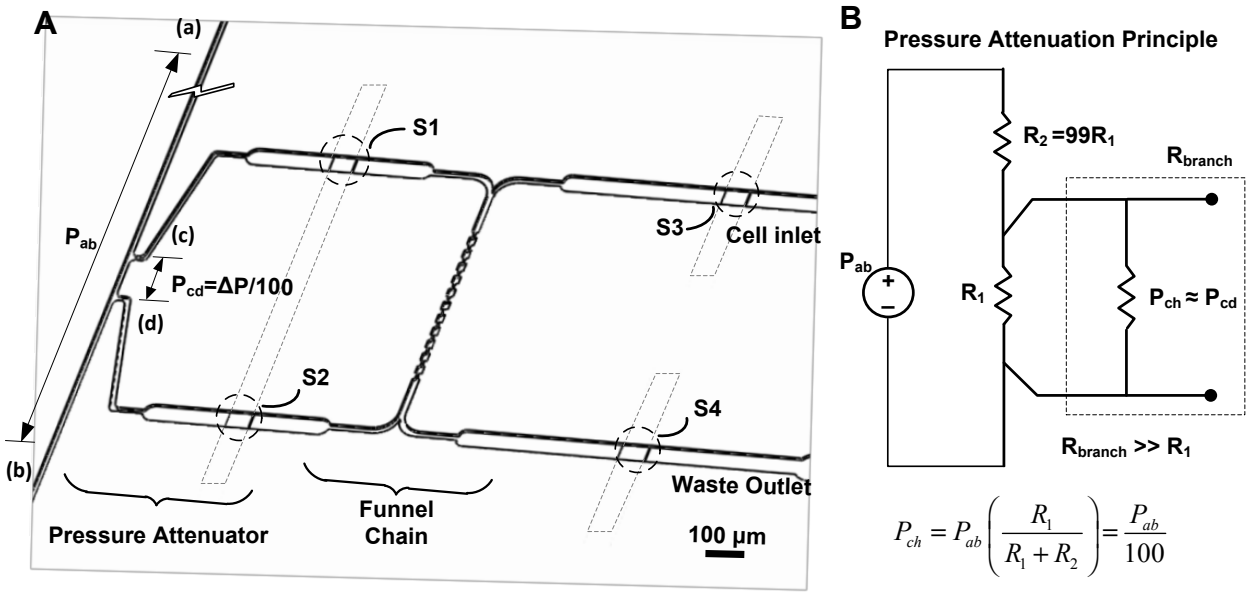

Fig. 2 *(A) Design of the microfluidic device for deforming single cells using precisely controlled pressure. (B) Fluidic circuitry for the pressure attenuation part of the device.*

MATERIAL AND METHODS

Device Fabrication

Molds of the flow layer and control layer microstructures were fabricated using a photolithographic process. The funnel chain part of the flow layer mold shown in Fig. 2 was fabricated using SU-8 photoresist (MicroChem, Newton, MA, USA), whereas the pressure attenuator and cell inlet parts of the flow layer mold were made from SPR 220-7.0 photoresist (MicroChem). The control layer mold was made entirely of SPR 220-7.0. Patterns for flow and control layers were drawn using AutoCAD. Optical photomask for the SU-8 microstructures was manufactured using laser direct-write by Advance Reproductions (North Andover, MA, USA). Optical photomasks for the SPR microstructures were manufactured on transparency films by CAD/Art Services (Bandon, OR, USA).

SU-8 microstructures were fabricated on 100 mm diameter silicon wafers. Each wafer was initially dehydrated by baking on a hotplate at 200°C for 5 minutes. Several SU-8 varieties and spin speeds were used to produce the desired flow channel thicknesses required for different cell types. Processing parameters are listed in Table 1. After spin-coating, each wafer was baked at 95°C on the hotplate for 20 minutes; exposed in a mask aligner (Canon) for 30 to 40 seconds; and then baked at 65°C for 1 minute, 95°C for 1.5 minutes, and then 65°C for 1 minute. Each wafer was then developed using SU-8 developer (MicroChem). Finally, in order to stabilize the SU-8 microstructures, the wafers were baked on a hot plate where the bake temperature was gradually ramped from 40°C to 200°C, held at 200°C for one hour, and then gradually cooled to 40°C.

Table 1 *Spin speeds used to produce various thicknesses of SU-8 films.*

Film Thickness (µm)	SU-8 Type	Spin Speed (rpm)
8.3	SU-8 2007	2000
7	SU-8 3005	3000
12	SU-8 3010	1500
17	SU-8 2025	4000

Following fabrication of the SU-8 microstructure, a layer of SPR 220-7.0 photoresist was added to create microvalves in the flow channels [40]. SPR 220-7.0 photoresist was spin-coated on the wafer at 600 rpm for 50 seconds followed by edge-bead removal. Each wafer was then baked at 65°C for 1 minute, 95°C for 2 minutes, and then 65°C for 1 minute. Next, the SPR mask was aligned with the SU-8 pattern and exposed for 4 minutes in intervals of 30 seconds. After waiting for 30 minutes, each wafer was then

developed using MF-319 developer (MicroChem). The control layer microstructure was fabricated in SPR using the same procedures as described above.

The silicon molds were replicated in a polyurethane-based plastic (Smooth-Cast 310, Smooth-On, Easton, PA, USA) using the process described by Desai *et al.* [41]. The microfluidic devices were fabricated by casting PDMS into the polyurethane mold and assembled using multilayer soft-lithography [40, 42] with flow layer on top of the control layer. Sample and control inlets were punched manually using 0.5 mm diameter punches (Technical Innovations, Angleton, TX, USA). Finally, the double layer PDMS devices were bonded to a standard glass slide following air plasma activation (Harrick Plasma, Ithaca, NY, USA).

Cell Sample Preparation

Whole blood was collected from healthy donors with informed consent into 6 ml tubes containing EDTA as anti-coagulant. Neutrophils were isolated from whole blood by gradient density centrifugation using Histopaque solutions 1077 and 1119 (Sigma-Aldrich, St. Louis, MO, USA) [43]. 3 ml of Histopaque 1077 was carefully layered on the top of 3 ml of Histopaque 1199 in a 15 ml centrifuge tube. Next, 6 ml of whole blood was added on top of the layered Histopaque 1077 and 1199. The tube was then centrifuged at 700g for 30 min without braking at 24 °C. Two layers of cells, consisting of lymphocytes and neutrophils, were transfered into separate 15 ml centrifuge tubes containing 10ml of HBSS without Ca^{2+} and Mg^{2+} solution (Invitrogen, Grand Island, NY, USA). The collected cell suspensions were centrifuged at 300 g for 10 min. After removing the supernatant, the pelleted cells were washed twice using HBSS.

L1210 Mouse Lymphoma cells were cultured in RPMI 1640 medium containing 10% (v/v) fetal bovine serum and 1% penicillin/streptomycin (Invitrogen) at 37˚C in a humidified atmosphere containing 5% CO_2. RT4 cancer cells were cultured in MEM with 10% (v/v) fetal bovine serum, 1% L-glutamine, 1% MEM Non-Essential Amino Acids, 1% Sodium Pyruvate (Invitrogen) under the same condition as L1210 Mouse Lymphoma cells.

Prior to testing, all cell samples were suspended in phosphate buffered saline with 5% bovine serum albumin. Microfluidic devices were filled with the same buffer solution and incubated for 30 minutes to prevent non-specific adsorption to the channel surfaces. After sample cells are infused into the microfluidic device, the diameter of each test cell was observed using a 20X microscope objective (Nikon) and measured using NIS-Elements software (Nikon).

Experimental Apparatus

Two pneumatic pressure control systems were used to control fluid flow in the microfluidic devices. The first system is a custom-made pressure controller designed to supply pressure from 0 to 4000 mbar, adjustable using manual pressure regulators (Omega, Laval, QC, Canada) and gauges (McMaster-Carr, Cleveland, OH, USA). On/off pressure control is enabled using solenoid valves (Pneumadyne, Plymouth, MN, USA) controlled by MOSFET switches and a MSP430 microcontroller (Texas Instruments, Dallas, TX, USA) integrated on a custom printed circuit board. These components are controlled digitally through the microcontroller via a custom Visual Basic user interface. The second pressure control system is the MFCS-4C system purchased from Fluigent (Paris, France). This system supplies precise pressure with a resolution of 25 mbar (25 Pa) and a range of 1000 mbar using closed-loop control.

Experimental Procedure

To measure the threshold pressure to deform single cells through each funnel constriction, we first introduce each cell through the inlet with valves S3 and S4 open, and S1 and S2 closed. The pressure applied at the inlet controls the flow rate of the sample. Cell samples are typically suspended at a concentration of ~10^6 cells/ml to ensure cells being introduced into the device without excessive waiting time or with multiple cells appearing in the funnel chain simultaneously. Once a single cell enters the funnel chain area, S1 and S2 are opened at the same time as S3 and S4 are closed in order to apply an attenuated pressure across the chain of funnel constrictions. The applied pressure is gradually increased to measure the threshold deformation pressure. Initially, a relatively low pressure (~10 Pa after attenuation) is applied to move the cell to the mouth of the funnel. Once the cell arrives at the funnel, the pressure is then gradually increased until the cell is rapidly ejected through the funnel pore. This threshold pressure is recorded and used to calculate the intrinsic deformability of the cell. After ejecting through the pore, the cell is given a few seconds to relax to its original shape before going through another pore. Measured pressure values are deemed valid as long as the cell shows no visible signs of damage, permanent change in shape, or activation in the case of neutrophils.

Results and Discussion

Modeling

To obtain an intrinsic (*i.e.* size-independent) measure of cell deformability, we modeled the cell using the liquid-drop model, which assumes a liquid-filled sac with constant volume, and that cell deformability is attributed to a persistent cortical tension in the cell membrane [18]. When each cell is

constrained in the funnel-shaped constriction, the deformed volume of the cell can be divided into a three sections: a leading ellipsoid, an internal section in contact with the constriction, and a trailing ellipsoid (Fig. 3A). The pressure difference required to quasi-statically form the leading surface can be determined using the Laplace-Young equation [18],

$$P_{cell} - P_{lead} = T_c \left(\frac{1}{R_{a1}} + \frac{1}{R_{a2}} \right) \quad (1)$$

where R_{a1} and R_{a2} is the in-plane and out-of-plane radius of curvature, and T_c is the cortical tension of the cell membrane, which describes the intrinsic deformability of the cell. Similarly, the pressure difference required to form the trailing surface can be determined using

$$P_{cell} - P_{trail} = T_c \left(\frac{1}{R_{b1}} + \frac{1}{R_{b2}} \right) \quad (2)$$

where R_{b1} and R_{b2} is the in-plane and out-of-plane radius of curvature of the trailing surface. Subtracting (3) from (2) gives an expression for the pressure difference across a funnel constriction, P_{funnel},

$$P_{funnel} = P_{trail} - P_{lead} = T_c \left(\frac{1}{R_{a1}} + \frac{1}{R_{a2}} - \frac{1}{R_{b1}} - \frac{1}{R_{b2}} \right) \quad (3)$$

When a cell is sufficiently constrained by the thickness of the planar microchannel, the out-of-plane radii of curvature are identical and equal to $h_0/2$, as shown in Fig. 3B. Therefore, Equation 3 simplifies to

$$\Delta P = T_c \left(\frac{1}{R_{a1}} - \frac{1}{R_{b1}} \right) \quad (4)$$

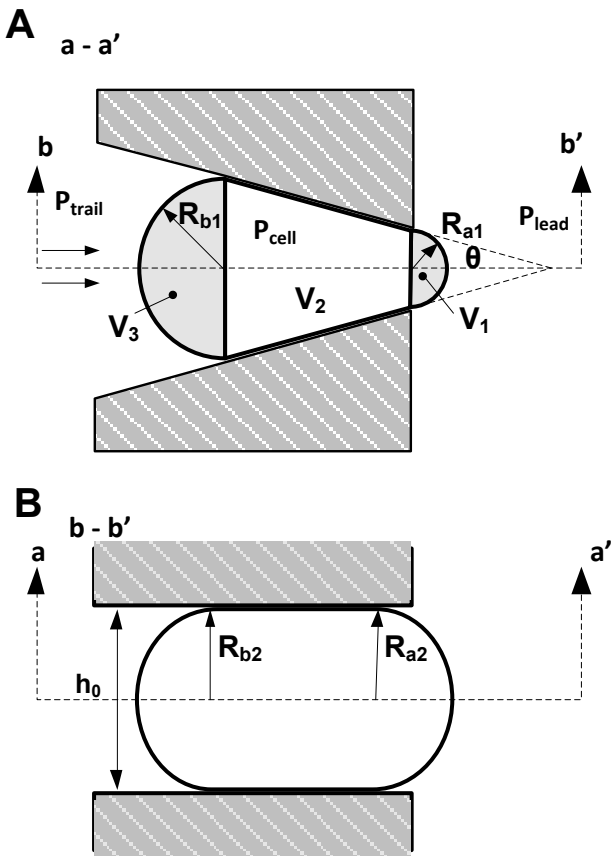

Fig. 3 *(A) Coronal (XY plane according to axes in Fig. 1) cross-section of a single cell being deformed in a funnel constriction. (B) Sagittal (YZ plane) cross-section.*

Similar to whole cell MPA experiments, we measured the threshold deformation pressure by slowly increasing the applied pressure difference until each test cell is rapidly pulled across the constriction. This behavior is known as a Haines' jump [44] and occurs when the leading edge radius of the cell becomes one-half of the pore size, W_0 [18]. Therefore, the pressure required for the test cell to transit through the constriction can be predicted using Equation 4 from the R_{a1} and R_{b1} values that result from the constraint provided by the funnel. Specifically, we model the geometry of the cell at the critical point of deformation in 3 parts as shown in Fig. 3A. V_1 and V_3 are modeled as half-ellipsoids with in-plane radii R_{a1} and R_{b1}, as well as out-of-plane radii $R_{a2} = R_{a2} = h_0/2$. The volume of the middle section, V_2, can be estimated by assuming the cell conforms entirely to fill a section of the funnel. This assumption is reasonable as long as the test cells undergo significant deformation and thereby conforms to the shape of the funnel constriction. In our case, 8 µm diameter neutrophil is typically deformed using funnel constrictions with W_0 from 4 to 1.2 µm. The statement of volume conservation for determining R_{b1} can therefore be expressed as

$$\frac{4}{3}R_0^3 = \frac{h_0}{3}R_{a1}^2 + \frac{h_0}{3}R_{b1}^2 + \Delta x \frac{h_0}{\pi}\sum_i W(i) \quad (5)$$

where R_0 is the undeformed cell radius and $W(i)$ is the profile of the funnel. At the critical point of deformation, $R_{a1} = W_0/2$, and R_{b1} can be determined by numerically solving Equation 5 for each cell. The cortical tension for each cell can then be calculated using Equation 4.

Neutrophils

Neutrophils are often used as a standard test cell in classical MPA experiments [10-13]. We tested neutrophils extracted from healthy donors with informed consent using devices with h_0 = 8.3 µm. Threshold deformation pressures were measured using funnels with pore size ranging from 4 µm down to 1.2 µm. Fig. 4 shows example microscopy images from the deformation of a single neutrophil, including initial approach, deformation, critical point, and ejection through the funnel. Each cell is deformed through 6 or 7 constrictions ranging from 4 µm down to 1.2 µm. In total, we made ~80 measurements on 12 neutrophils in a single device. All of the tested cells appeared to remain intact and showed no signs of membrane leakage or rupture. Furthermore, all tested neutrophils appeared to remain in a passive state and showed no morphological changes that are characteristic of activation. To determine the cortical tension of neutrophils, we plotted the measured deformation pressure as a function of ($1/R_{a1}$ - $1/R_{b1}$) as shown in Fig. 5A. From Equation 4, the cortical tension is the slope of the linear fit line.

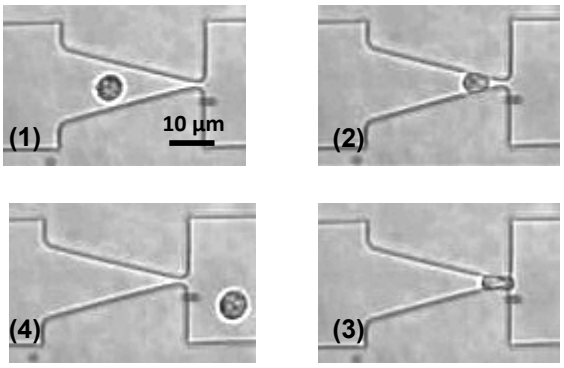

Fig. 4 *Micrographs of a single neutrophil being deformed through a funnel constriction: (1) initial approach, (2) deformation, (3) critical point, and (4) ejection through the funnel.*

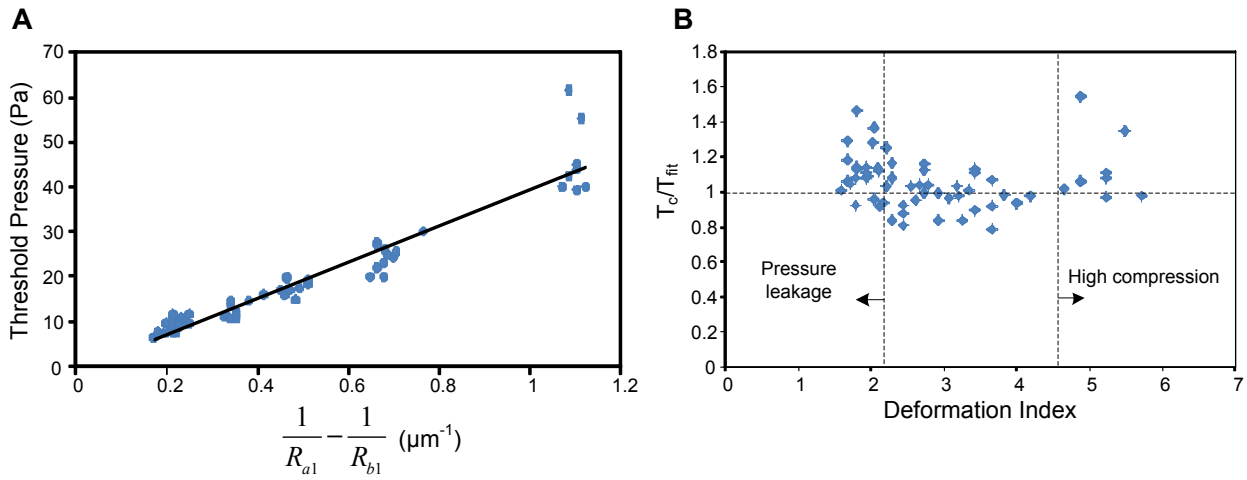

Fig. 5 *(A) Measured threshold pressure as a function $1/R_{a1}$ - $1/R_{b1}$. (B) Residue of the linear fit plotted as the ratio of the calculated cortical tension (T_c) and the fitted cortical tension (T_{fit}) as a function of the cell deformation index as defined in Equation 6.*

To study errors associated with our measurement process, we plot the residue of the linear fit as a function of cell deformation index (DI) in Fig. 5B. DI is defined as the ratio of the cross-sectional area of the cell and of the funnel opening where

$$DI = \frac{A_{cell}}{A_{funnel}} = \frac{\pi R_0^2}{h_0 W_0} \qquad (6)$$

The residue of the linear fit in Fig. 5A is shown as the ratio of the calculated cortical tension from each measured neutrophil and the average value determined using the linear fit. As indicated in Fig. 5B, cortical tension values measured using a median deformation index (4.5 > DI > 2.2) were independent of deformation index, whereas measurements at both large and small deformation indices resulted in cortical tension values greater than the fitted mean value.

At large DI values (DI > 4.5), deviations from the model likely result from excessive deformation, where internal cellular structures, such as the nucleus and cytoskeleton, begin contributing to the measured cell deformability. Similar characteristics have been observed in previous MPA studies [13, 14, 45], where the measured cortical tension increases as cells are aspirated into smaller pipettes using greater pressures.

At small DI values (DI < 2.2), deviations from the model likely result from leaked fluid flow when the cell insufficiently conforms to the rectangular funnel constriction. Since our measurement technique relies on being able to create an effective seal as each cell is deformed into a funnel constriction, a leaky seal

would require greater pressures to be applied to the funnel chain in order to impart the same deformation force to each test cell. As a result, the calculated cortical tension based on these measurements over-estimates the actual value as shown in Fig. 6.

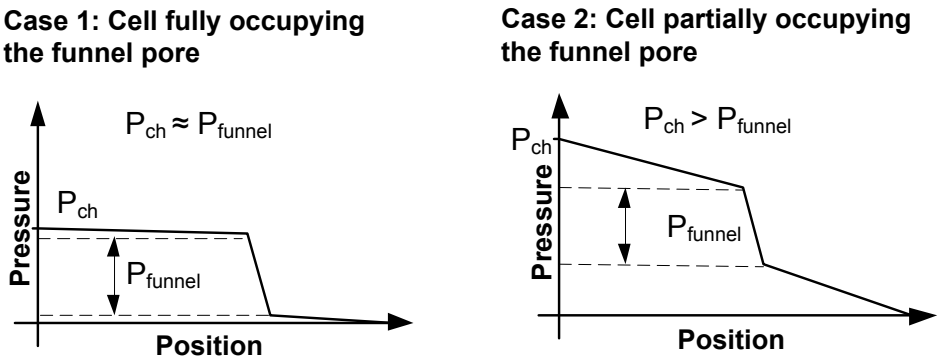

Fig. 6 *Potential measurement error resulting from leaked fluid around the cell at small DI values.*

Based on the results in Fig. 5B, we can develop a heuristic for qualifying cell deformability measurements made using our system. Specifically, measurements are considered valid when the deformation index is between 2.2 and 4.5. Analyzing neutrophil data in this range, we find the average neutrophil cortical tension to be 37.0 ± 4.8 pN/μm. This result is consistent with values reported in previous MPA studies as shown in Fig. 7A, and the standard deviation from previous measurements have been included where available [10, 13, 24, 37]. The coefficient of variation (CV) of our measurement is 0.13, which is inline with the best available results obtained using MPA.

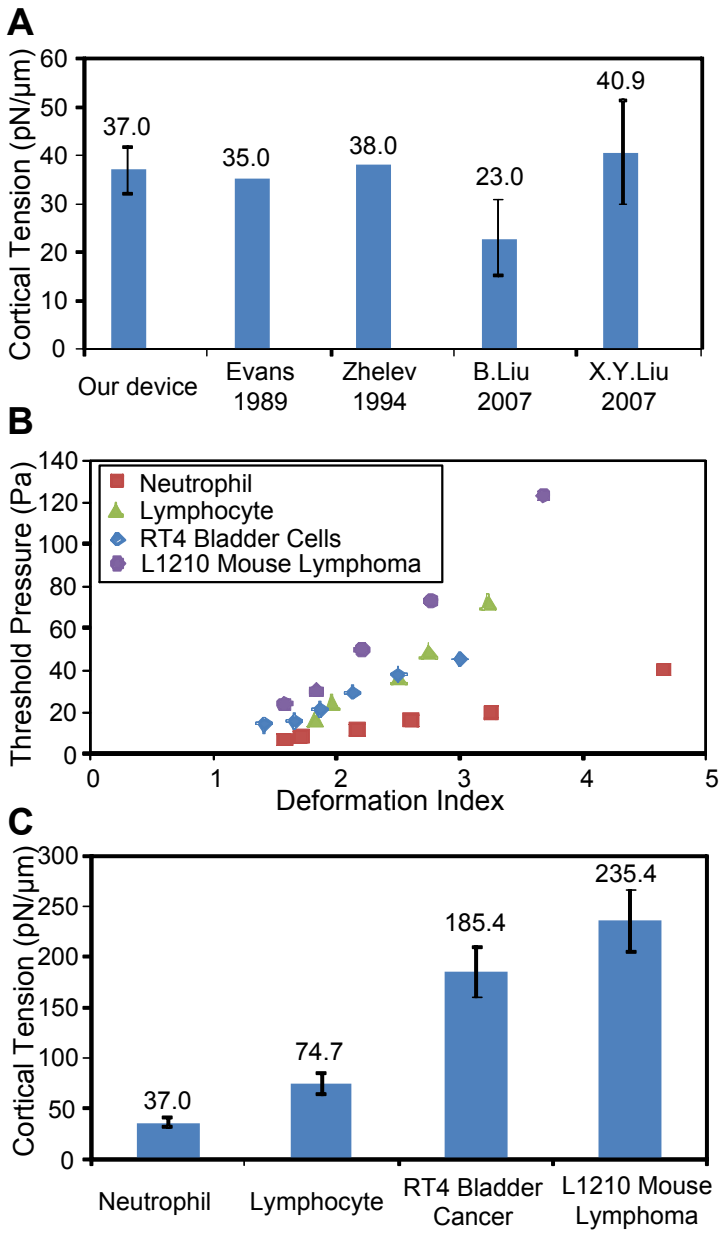

Fig. 7 *(A) Comparison of the mean cortical tension of human neutrophils measured using our device with others measured using MPA. Error bars indicating standard deviation are shown where available. (B) Example threshold pressures measured as a function of DI from each of the four tested cell types. (C) Comparison of the measured cortical tension from four different cell types.*

Other Cell Types

To evaluate the utility of our device, we measured the deformability of four cell types with distinct mechanical properties, including human neutrophils, human lymphocytes, RT4 human bladder cancer cells, and L1210 mouse lymphoma cells. Separate versions of the microfluidic device were fabricated to customize the thickness of the funnel channel for each cell type. Since photolithographic

microfabrication is a planar process, the thickness of the microchannels must be selected *a priori* for each cell type. The optimal device geometry, including funnel pore size (W_0) and microchannel thickness (h_0) is shown in Table 1. These parameters were selected based on the size distribution of each cell type in order to obtain DI values between 2.2 and 4.5 to minimize measurement errors. Structural integrity of was preserved for almost all of the tested cells. On rare instances, a few L1210 mouse lymphoma cell were observed to lyse when compressed at DI > 4.5. Measurement data from these cells were discarded and not used in further analysis.

Table 2 *Microchannel thicknesses used to test different cell types*

Cell Type	Cell Diameter (μm)	Channel Thickness h_0 (μm)	DI range
Neutrophils	8.2 ± 0.7	8.3	2.2 – 4.5
Lymphocytes	7.0 ± 0.8	7.0	2.5 – 3.5
RT4 Bladder Cancer	18.0 ± 2.0	17.0	2.2 – 3.0
L1210 Mouse Lymphoma	12.8 ± 0.5	12.0	2.5 – 4.0

Example threshold deformation pressures from each of the four types are plotted as a function of DI in Fig. 7B. The data shown are from example cells where the cell diameter is approximately the same as the mean diameter for the cell population. These results show that neutrophils require the least amount of deformation pressure, while mouse lymphoma require the most. Fig. 7C compares the cortical tensions between the four measured cell types. Each data point shows the mean and standard deviation of the result from 12 to 20 cells. Lymphocytes are approximately twice as rigid as neutrophils. RT4 bladder cancer cells and L1210 mouse lymphoma cells are approximately 5X and 6.5X more rigid than human lymphocytes. These results are not surprising given that cancer cells generally have a larger nucleus and well-developed cytoskeleton compared to leukocytes.

The greater rigidity of L1210 cells compared to RT4 cells is likely due to their greater nucleus-to-cytoplasm (N:C) ratio. L1210 cells contain a nucleus that fills more than half of the cytosol, whereas RT4 cells contain a nucleus that fills approximately one-third of the cytosol. The nucleus-to-cytoplasm ratio of these cell types were quantified by staining the nucleus using the Hoechst stain (Thermo Scientific) followed by measurement using a fluorescent microscope. The nucleus-to-cytoplasm (N:C) ratio is

defined as the ratio of the cross-sectional area of the nucleus divided by the cross-sectional area of the cytosol. We measured at least 30 cells of each type and found the N:C value to be 0.528 ± 0.076 and 0.344 ± 0.074 for L1210 and RT4 respectively.

Deformability of lymphocytes, RT4 bladder cancer cells, and L1210 mouse lymphoma cells have not been reported previously. As a point of reference, the cortical tension of mouse fibroblast (L929) [46], Jurkat cells [47], and human macrophages (J774) [14] were found to be 413.6 ± 15.2 , 21 ± 13, and 140 respectively. These results are within an order of magnitude of our measured results for related cell types.

Finally, we studied the repeatability of our measurement technique using L1210 mouse lymphoma cells. A single cell of diameter of 15.6 µm was deformed through funnel constrictions with pore sizes of 9.6, 8.7, 7.7, and 6.8 µm. Threshold deformation pressures were measured 3 ~ 5 times per constriction. The measured threshold deformation pressures from each constriction were repeatable within 10% of the mean.

Summary and Conclusions

Micropipette aspiration is a versatile method for measuring the deformability of individual cells. We developed a microfluidic device to perform these measurements using a nearly identical approach, but leverages recent advances in microfluidics and microfabrication to improve ease-of-use in the following ways while preserving measurement precision. First, MPA experiments operate in an open environment where liquid from the sample is continuously evaporating. This fluid loss presents a drifting baseline pressure that must be periodically recalibrated in order to generate precise pressure differences. Our microfluidic device is a closed system impervious to evaporative losses, and thereby improves the accuracy of the measured pressure. The use of microfluidic networks to create a pressure attenuator further reduces the specifications required of external pressure controllers. Second, MPA experiments require the use of a 3-axis micromanipulator to localize the pipette tip to the surface of a target cell. This process not only requires specialized equipment, but also considerable experimental skills, which further adds to the cost and difficulty of micropipette aspiration studies. Finally, MPA experiments typically use a single pipette to study a small population of cells from a sample. Since significant cell size variations exist within a sample or a phenotype, the diameter of the pipette orifice may not be optimal for each

cell. Our device contains multiple constrictions that cover a range of sizes, thereby enabling the optimal constriction to be selected for each cell type.

A challenge associated with our technique is the need to match of the device channel opening with the size of the sample cells to produce a DI between 2.2 and 4.5. While this range is sufficiently large to allow cells of one phenotype to be tested using a single device, different cell types typically require different device geometries. Additionally, the device presented is capable of testing ~30 cells per hour, with 15 minutes of preparation time. While this level of throughput is better than traditional MPA, in order for this device to be more useful in clinical situations, automated testing combined with greater throughput or reduced testing time would be more desirable.

References

[1] J. Guck, *et al.*, "Optical deformability as an inherent cell marker for testing malignant transformation and metastatic competence," *Biophysical Journal,* vol. 88, pp. 3689-3698, May 2005.

[2] S. Suresh, "Biomechanics and biophysics of cancer cells," *Acta Materialia,* vol. 55, pp. 3989-4014, Jul 2007.

[3] S. Suresh, *et al.*, "Connections between single-cell biomechanics and human disease states: gastrointestinal cancer and malaria," *Acta Biomaterialia,* vol. 1, pp. 15-30, Jan 2005.

[4] H. A. Cranston, *et al.*, "Plasmodium-Falciparum Maturation Abolishes Physiologic Red-Cell Deformability," *Science,* vol. 223, pp. 400-403, 1984.

[5] G. B. Nash, *et al.*, "Abnormalities in the Mechanical-Properties of Red Blood-Cells Caused by Plasmodium-Falciparum," *Blood,* vol. 74, pp. 855-861, Aug 1 1989.

[6] G. Y. H. Lee and C. T. Lim, "Biomechanics approaches to studying human diseases," *Trends in Biotechnology,* vol. 25, pp. 111-118, Mar 2007.

[7] W. R. Jones, *et al.*, "Alterations in the Young's modulus and volumetric properties of chondrocytes isolated from normal and osteoarthritic human cartilage," *Journal of Biomechanics,* vol. 32, pp. 119-127, Feb 1999.

[8] E. A. Evans, "New Membrane Concept Applied to Analysis of Fluid Shear-Deformed and Micropipet-Deformed Red Blood-Cells," *Biophysical Journal,* vol. 13, pp. 941-954, 1973.

[9] R. P. Rand and A. C. Burton, "Mechanical Properties of Red Cell Membrane .I. Membrane Stiffness + Intracellular Pressure," *Biophysical Journal,* vol. 4, pp. 115-&, 1964.

[10] E. Evans and A. Yeung, "Apparent Viscosity and Cortical Tension of Blood Granulocytes Determined by Micropipet Aspiration," *Biophysical Journal,* vol. 56, pp. 151-160, Jul 1989.

[11] D. Needham and R. M. Hochmuth, "Rapid Flow of Passive Neutrophils into a 4 Mu-M Pipette and Measurement of Cytoplasmic Viscosity," *Journal of Biomechanical Engineering-Transactions of the Asme,* vol. 112, pp. 269-276, Aug 1990.

[12] M. A. Tsai, *et al.*, "Passive Mechanical-Behavior of Human Neutrophils - Power-Law Fluid," *Biophysical Journal,* vol. 65, pp. 2078-2088, Nov 1993.

[13] D. V. Zhelev, *et al.*, "Role of the Membrane Cortex in Neutrophil Deformation in Small Pipettes," *Biophysical Journal,* vol. 67, pp. 696-705, Aug 1994.

[14] J. Lam, *et al.*, "Baseline Mechanical Characterization of J774 Macrophages," *Biophysical Journal,* vol. 96, pp. 248-254, Jan 2009.

[15] M. Sato, *et al.*, "Micropipette Aspiration of Cultured Bovine Aortic Endothelial-Cells Exposed to Shear-Stress," *Arteriosclerosis,* vol. 7, pp. 276-286, May-Jun 1987.

[16] M. Sato, *et al.*, "Application of the Micropipette Technique to the Measurement of Cultured Porcine Aortic Endothelial-Cell Viscoelastic Properties," *Journal of Biomechanical Engineering-Transactions of the Asme,* vol. 112, pp. 263-268, Aug 1990.

[17] J. Y. Tinevez, *et al.*, "Role of cortical tension in bleb growth," *Proc. Natl. Acad. Sci. U.S.A.,* vol. 106, pp. 18581-18586, Nov 3 2009.

[18] R. M. Hochmuth, "Micropipette aspiration of living cells," *Journal of Biomechanics,* vol. 33, pp. 15-22, Jan 2000.

[19] E. A. Evans and R. M. Hochmuth, "Membrane Viscoelasticity," *Biophysical Journal,* vol. 16, pp. 1-11, 1976.

[20] A. Yeung and E. Evans, "Cortical shell-liquid core model for passive flow of liquid-like spherical cells into micropipets," *Biophysical Journal,* vol. 56, pp. 139-149, Jul 1989.

[21] E. Evans and B. Kukan, "Passive material behavior of granulocytes based on large deformation and recovery after deformation tests," *Blood,* vol. 64, pp. 1028-1035, 1984.

[22] V. Heinrich and W. Rawicz, "Automated, high-resolution micropipet aspiration reveals new insight into the physical properties of fluid membranes," *Langmuir,* vol. 21, pp. 1962-1971, Mar 1 2005.

[23] J. L. Drury and M. Dembo, "Hydrodynamics of micropipette aspiration," *Biophysical Journal,* vol. 76, pp. 110-128, Jan 1999.

[24] X. Y. Liu, *et al.*, "Real-time high-accuracy micropipette aspiration tor characterizing mechanical properties of biological cells," in *Proceedings of the 2007 Ieee International Conference on Robotics and Automation, Vols 1-10*, ed, 2007, pp. 1930-1935.

[25] S. Gabriele, *et al.*, "A simple microfluidic method to select, isolate, and manipulate single-cells in mechanical and biochemical assays," *Lab on a Chip,* vol. 10, pp. 1459-1467, 2010.

[26] H. W. Hou, *et al.*, "Deformability study of breast cancer cells using microfluidics," *Biomedical Microdevices,* vol. 11, pp. 557-564, Jun 2009.

[27] M. J. Rosenbluth, *et al.*, "Analyzing cell mechanics in hematologic diseases with microfluidic biophysical flow cytometry," *Lab on a Chip,* vol. 8, pp. 1062-1070, 2008.

[28] H. Bow, *et al.*, "A microfabricated deformability-based flow cytometer with application to malaria," *Lab on a Chip,* vol. 11, pp. 1065-1073, 2011.

[29] G. Guan, *et al.*, "Size-Independent Deformability Cytometry with Active Feedback Control of Microfluidic Channels," presented at the 15th International Conference on Miniaturized Systems for Chemistry and Life Sciences, Seattle, WA, USA, 2011.

[30] J. A. Chen, *et al.*, "A microfluidic device for simultaneous electrical and mechanical measurements on single cells," *Biomicrofluidics,* vol. 5, Mar 2011.

[31] W. Kim and A. Han, "A Micro-Aspirator Chip Using Vacuum Expanded Microchannels for High-throughput Mechanical Characterization of Biological Cells," presented at the The 14th International Conference on Miniaturized Systems for Chemistry and Life Sciences (MicroTAS), Groningen, The Netherlands, 2010.

[32] S. C. Gifford, *et al.*, "A detailed study of time-dependent changes in human red blood cells: from reticulocyte maturation to erythrocyte senescence," *British Journal of Haematology,* vol. 135, pp. 395-404, Nov 2006.

[33] T. Herricks, *et al.*, "Deformability limits of Plasmodium falciparum-infected red blood cells," *Cellular microbiology,* vol. 11, pp. 1340-1353, 2009.

[34] A. M. Forsyth, *et al.*, "The dynamic behavior of chemically "stiffened" red blood cells in microchannel flows," *Microvascular Research,* vol. 80, pp. 37-43, Jul 2010.

[35] S. C. Hur, *et al.*, "Deformability-based cell classification and enrichment using inertial microfluidics," *Lab on a Chip,* vol. 11, pp. 912-920, 2011.

[36] S. S. Lee, *et al.*, "Extensional flow-based assessment of red blood cell deformability using hyperbolic converging microchannel," *Biomedical Microdevices,* vol. 11, pp. 1021-1027, Oct 2009.

[37] B. Liu, *et al.*, "Effect of temperature on tether extraction, surface protrusion, and cortical tension of human neutrophils," *Biophysical Journal,* vol. 93, pp. 2923-2933, Oct 2007.

[38] S. M. M. Quan Guo, and Hongshen Ma, "Deterministic microfluidic ratchet based on the deformation of individual cells," *Phys. Rev. E,* vol. 83, 2011.

[39] Quan Guo, *et al.*, "Microfluidic biomechanical assay for red blood cells parasitized by *Plasmodium falciparum*," *Lab on a Chip,* 2012.

[40] M. A. Unger, *et al.*, "Monolithic microfabricated valves and pumps by multilayer soft lithography," *Science,* vol. 288, pp. 113-116, Apr 7 2000.

[41] S. P. Desai, *et al.*, "Plastic masters-rigid templates for soft lithography," *Lab on a Chip,* vol. 9, pp. 1631-1637, 2009.

[42] V. Studer, *et al.*, "Scaling properties of a low-actuation pressure microfluidic valve," *Journal of Applied Physics,* vol. 95, pp. 393-398, Jan 2004.

[43] M. Freltas, *et al.*, "Isolation and activation of human neutrophils in vitro. The importance of the anticoagulant used during blood collection," *Clinical Biochemistry,* vol. 41, pp. 570-575, May 2008.

[44] W. B. Haines, "Studies in the physical properties of soil V The hysteresis effect in capillary properties, and the modes of moisture distribution associated therewith," *Journal of Agricultural Science,* vol. 20, pp. 97-116, Jan 1930.

[45] D. Needham and R. M. Hochmuth, "A sensitive measure of surface stress in the resting neutrophil," *Biophysical Journal,* vol. 61, pp. 1664-1670, Jun 1992.

[46] J. Y. Tinevez, *et al.*, "Role of cortical tension in bleb growth," *Proceedings of the National Academy of Sciences of the United States of America,* vol. 106, pp. 18581-18586, Nov 2009.

[47] M. J. Rosenbluth, *et al.*, "Force microscopy of nonadherent cells: A comparison of leukemia cell deformability," *Biophysical Journal,* vol. 90, pp. 2994-3003, Apr 2006.